Specific collagens maintain the cuticle permeability barrier in Caenorhabditis elegans

Sandhu, Anjali; Badal, Divakar; Sheokand, Riya; Tyagi, Shalini; Singh, Varsha

Published in:
Genetics

DOI:
10.1093/GENETICS/IYAA047

Publication date:
2021

OXFORD GENETICS

GENETICS, 2021, 217(3), iyaa047
DOI: 10.1093/genetics/iyaa047
Advance Access Publication Date: 29 January 2021
Investigation

Specific collagens maintain the cuticle permeability barrier in *Caenorhabditis elegans*

Anjali Sandhu,[1] Divakar Badal,[2] Riya Sheokand,[1] Shalini Tyagi,[1] and Varsha Singh [1,2,3,*]

[1]Department of Molecular Reproduction, Development and Genetics, Indian Institute of Science, Bangalore 560012, India
[2]Center for Biosystems Science and Engineering, Indian Institute of Science, Bangalore 560012, India
[3]Lead contact

*Corresponding author: varsha@iisc.ac.in

Abstract

Collagen-enriched cuticle forms the outermost layer of skin in nematode *Caenorhabditis elegans*. The nematode's genome encodes 177 collagens, but little is known about their role in maintaining the structure or barrier function of the cuticle. In this study, we found six permeability determining (PD) collagens. Loss of any of these PD collagens—DPY-2, DPY-3, DPY-7, DPY-8, DPY-9, and DPY-10—led to enhanced susceptibility of nematodes to paraquat (PQ) and antihelminthic drugs- levamisole and ivermectin. Upon exposure to PQ, PD collagen mutants accumulated more PQ and incurred more damage and death despite the robust activation of antioxidant machinery. We find that BLMP-1, a zinc finger transcription factor, maintains the barrier function of the cuticle by regulating the expression of PD collagens. We show that the permeability barrier maintained by PD collagens acts in parallel to FOXO transcription factor DAF-16 to enhance survival of insulin-like receptor mutant, *daf-2*. In all, this study shows that PD collagens regulate cuticle permeability by maintaining the structure of *C. elegans* cuticle and thus provide protection against exogenous toxins.

Keywords: Caenorhabditis elegans; collagens; dumpy; BLMP-1; cuticle; permeability; hypodermis; paraquat; oxidative stress; survival

Introduction

Skin isolates an organism from its environment. The composition and the structure of skin can vary considerably from being a multilayered, complex organ in humans to single-layered in *Caenorhabditis elegans*. The skin protects the organism from dehydration, from infections and it is thought to act as a physical barrier against environmental toxins. Although the phylum Nematoda diverged from vertebrates very early in evolution, *C. elegans* skin can also respond to injury by activating wound healing signaling pathways, to hyperosmotic stress by up-regulating glycerol synthesis pathway, and to pathogen invasion by triggering production of antimicrobial peptides, as also seen in vertebrates suggesting conserved function of the skin (Lamitina *et al.* 2004; Pujol *et al.* 2008a, 2008b; Chisholm 2015; Taffoni and Pujol 2015).

Caenorhabditis elegans skin consists of two parts, hypodermis and cuticle. The hypodermis is a single cell layer that secretes the cuticle, the outermost layer of the skin (Cox *et al.* 1981a, 1981b). The cuticle of *C. elegans* is a flexible structure that helps in locomotion via attachment to muscle. The cuticle is composed of cross-linked collagens, glycoproteins, lipids, and additional insoluble proteins called cuticulins (Page and Johnstone 2007; Teuscher *et al.* 2019). As in vertebrate skin, collagens are the most abundant protein in the cuticle of nematodes (Johnstone 1994; Kramer 1994; Chisholm and Hsiao 2012). The cuticle collagens are similar to fibril-associated collagens with interrupted triple helices (FACIT) as the characteristic collagen Gly-X-Y repeats are interrupted by non-collagenous sequences (Johnstone 2000). There are 177 collagen-encoding genes in *C. elegans* genome, a majority of which are expressed, but their individual function in maintaining permeability to exogenous molecules and toxins is not well studied (Brenner 1974; Myllyharju and Kivirikko 2004; Lamitina *et al.* 2006; Teuscher *et al.* 2019). Loss- or reduction-of-function alleles of specific collagen can lead to body phenotypes described as dumpy (Dpy), roller (Rol), squat (Sqt), and blister (Bli) (Brenner 1974) suggesting that some collagens are crucial for maintaining the cuticle morphology (Schultz *et al.* 2014). Some collagens appear to have additional functions. Lack of cuticular collagen DPY-9 and DPY-10 causes induction of NLPs (neuropeptide-like proteins) and of glyceraldehyde-3-phosphate dehydrogenase (GPDH-1) linked to resistance against skin infection by coenocytic fungus *Drechmeria coniospora* and hyperosmotic stress respectively (Lamitina *et al.* 2006; Pujol *et al.* 2008b; Rohlfing *et al.* 2010; Schultz *et al.* 2014; Zugasti *et al.* 2014). These studies suggest that collagens can regulate stress response in the skin. Recent reports indicate that collagens can regulate the survival of worms on *Pseudomonas* under the control of G-protein-coupled receptor, neuropeptide receptor-8, or NPR-8 (Sellegounder *et al.* 2019).

Gene expression studies have suggested the involvement of several transcription factors in cuticle biogenesis and collagen expression. Knockdown of transcription factors such as SKN-1, HSF-1, BLMP-1, ELT-3, and ELT-1 leads to altered expression of

Received: February 15, 2020. **Accepted:** December 05, 2020

some collagens. SKN-1, a homolog of human Nuclear respiratory factor 1 (NRF1), dependent expression of collagens genes such as *col-10*, *col-13*, and *col-120* is required for enhanced longevity of *daf-2*, *C. elegans* ortholog of human insulin receptor (Ewald *et al.* 2015). The longevity and enhanced resistance to different stresses of *daf-2* mutants is also dependent on DAF-16, a FOXO transcription factor. However, the role of DAF-16 in collagen regulation remains unclear. Heat shock transcription factor HSF-1 positively regulates expression of *col-3*, *col-19*, *col-93*, *col-106*, *col-117*, *col-133*, *col-139*, *col-140*, and *col-181* in response to heat stress (Brunquell *et al.* 2016). *col-41* expression is controlled by GATA transcription factors ELT-1 and ELT-3 (Yin *et al.* 2015). BLMP-1, an ortholog of human PRDM1 (PR/SET domain 1), regulates expression of *bli-1* collagen positively while it regulates *rol-6*, *col-19*, *col-8*, and *rol-8* negatively (Hyun *et al.* 2016). TGF-beta signaling positively regulates expression of *col-165*, *col-89*, *col-167*, *col-61*, *col-118*, *col-72*, *col-182*, *col-33*, *col-174*, *col-51*, *col-3*, *col-43*, *col-44*, *col-48*, *col-176*, *col-84*, *col-184*, *col-113*, *col-153*, *col-112*, and *col-180* while it negatively regulates expression of *col-64* (Shaw *et al.* 2007). SMA-3, an ortholog of human SMAD1, positively regulate expression of *col-141* and negatively regulates expression of *col-41* and *rol-6* (Madaan *et al.* 2018). Despite the evidence that several transcription factors regulate collagen expression, identity of permeability determining (PD) collagens and their transcriptional regulators remains largely unknown.

While foraging for microbes in rotting vegetation in the soil, *C. elegans* can be exposed to a variety of toxins produced by microbes, and to herbicides present in farmland. The skin presents one of the largest surface areas to the environment and likely facilitates diffusion of toxins present in the nematode's habitat. This necessitates the existence of a permeability barrier in the cuticle. Although collagens are the most abundant proteins in the cuticle, role of collagens and their transcriptional regulators in maintaining the permeability barrier function of the cuticle, to protect from exogenous toxins, has not been studied.

In this study, we asked if collagens provide protection to worms by regulating the permeability barrier against exogenous toxins. We show that 6 cuticular collagens—DPY-2, DPY-3, DPY-7, DPY-8, DPY-9, and DPY-10—are required for maintaining cuticle structure and barrier function in *C. elegans*. Using environmental toxin paraquat (PQ) and anti-helminthic drugs levamisole and ivermectin, we show that PD cuticular collagens are essential for survival on exogenous toxins. We find that the BLMP-1 transcription factor is required for maintaining cuticle barrier and for survival on PQ by regulating the expression of PD collagens. In all, we establish an essential role for specific cuticular collagens in maintaining cuticle structure and permeability barrier function.

Materials and methods

Strains and reagents

Caenorhabditis elegans strains used in the study were wild-type N2 (Bristol), *dpy-4(e1166)*, *dpy-5(e61)*, *dpy-7(e88)*, *dpy-8(e1281)*, *dpy-9(e12)*, *dpy-10(e128)*, *bus-8(e2698)*, TP12 (COL-19::GFP), CL2166 (*Pgst-4::GFP*), and *daf-2(e1370)*. All strains were maintained at 20°C while *daf-2(e1370)* was maintained at 15°C. Reagents used for the study are—Paraquat (methyl viologen dichloride hydrate) (Sigma, Cat No. 856177), N-acetyl-L-cysteine (Sigma, Cat No. A7250), levamisole (Sigma, Cat No. 1916142), Ivermectin (Sigma, Cat No. 18898), and Hoechst 33258 (Sigma, Cat No. 94403).

RNAi interference

Systemic RNA interference by feeding was carried out as described (Fraser *et al.* 2000; Kamath *et al.* 2001). *Escherichia coli* strain HT115(DE3) expressing target double-stranded RNA that is homologous to a target gene was grown at 37°C, overnight, in LB broth containing carbenicillin (50 g/ml). Bacteria were plated onto NGM plates containing 50 g/ml carbenicillin and 5 mM isopropyl-D-thiogalactoside (IPTG) and incubated at 25°C for 12 h before use. Clones were confirmed by sequencing.

Survival assay

Worms were synchronized by allowing gravid worms to lay eggs for 4 h at 20°C (15°C for *daf-2*) on *E. coli*. To induce oxidative stress, a synchronized population of 50 young adult worms were exposed to 20 mM (Park *et al.* 2009) or 2 mM (Keaney *et al.* 2004) PQ on NGM plates and scored for survival every 6 h. Where indicated, plates also contained 5 mM N-acetyl cysteine (NAC) (Oh *et al.* 2015). For thermal stress, the synchronized population of worms were exposed to 32°C and scored for survival every 3 h (Beck and Rankin 1995). In pathogen survival assay, adult animals were exposed to *P. aeruginosa* PA14 at 25°C and scored for survival every 4 h (Styer *et al.* 2008).

Paralysis assay

For osmotic stress, the synchronized population of adult animals were exposed to 500 mM NaCl and scored for paralysis at 10 minutes (Wheeler and Thomas 2006). For levamisole stress, the synchronized population of adult animals were exposed to 125 μM levamisole and scored for paralysis at 30 minutes (Lewis *et al.* 1980). For ivermectin stress, the synchronized population of adult animals were exposed to 50 μM ivermectin and scored for paralysis at 8 minutes (Kass *et al.* 1980). Both the assays were performed at room temperature.

Pharyngeal pumping assay

Worms were synchronized by allowing gravid worms to lay eggs for 2–3 h at 20°C on *E. coli*. Young adult worms were exposed to 20 mM PQ or control. Videos were made for both, PQ treated and control, at 6 h of interval. Videos were analyzed using Adobe Premiere Pro CC.

Statistical analysis

All survival assays were plotted using the PRISM 5.01 (Kaplan–Meier method). Survival curves are considered significantly different than the control when *P*-values are <0.05 for Mantel–Cox test. Statistics for survival and paralysis are presented in Supplementary Table S2.

Cuticle permeability assay

Permeability was assessed by Hoechst 33258 staining in whole animals as described (Moribe *et al.* 2004). Hoechst 33258 staining screen with collagen RNAi animals was performed twice independently. Briefly, synchronized young adult worms were stained with 10 μg/ml Hoechst 33258 for 30 minutes at room temperature. Unbound stain was removed by washing with M9 buffer before visualization and imaging under the DAPI filter using Zeiss Apotome. All animals where we could observe at least 15 stained nuclei in the pharynx were scored as permeable. We scored 15–20 animals per condition per independent experiment.

Quantitative real-time PCR

Synchronized young adult nematodes were untreated or exposed to 20 mM PQ at 20°C for 6 h and then harvested. The animals

were harvested by washing the plates with M9 buffer and frozen in TRizol reagent at −80°C. RNA was extracted using RNeasy Plus Universal Mini Kit according to the manufacturer's instruction (Qiagen). cDNA was prepared using the iScript cDNA synthesis kit (BIO-RAD). qRT-PCR was conducted using the BIO-RAD TaqMan One-Step Real-time PCR protocol using SYBR Green fluorescence (BIO-RAD) on an Applied Biosystems QuantStudio 3 real-time PCR machine in 96-well plate format. Fifty nanograms of RNA were used for real-time PCR. About 10-µl reactions were set-up in two replicates and performed as outlined by the manufacturer (Applied Biosystems). Relative-fold changes were calculated using the comparative CT ($2^{-\Delta\Delta CT}$) method and normalized to actin-1 (Livak and Schmittgen 2001). Three or more biological replicates were used for qRT-PCR analysis.

Scanning electron microscopy

SEM samples were prepared as described previously (Shemer *et al.* 2004). Briefly, a synchronized population of young adult animals was fixed with 5% glutaraldehyde and 5% formaldehyde in 0.2 mM HEPES for 18–24 h then incubated with 2% osmium tetraoxide for 1–2 h. Animals were sequentially dehydrated with an increasing concentration of ethanol. Animals were mounted on glass coverslips and coated with gold before imaging. Imaging was done using a SIRION ultrahigh-resolution microscope.

Liquid chromatography-mass spectrometry

Synchronized animals were harvested and washed in distilled water. Animals in a packed volume of 500 µl were sonicated for 30 minutes at an amplitude of 60 on ice. The lysate was filtered using a 0.2 µm filter and the supernatant was analyzed. A 0.1% Ammonium formate aqueous solution (pH 3) was used as an aqueous solvent and acetonitrile was used as an organic solvent. About 15 µl of each sample was injected for analysis at a flow rate of 0.4 ml/minute with a total run time of 31 minutes on Bruker impact HT system. We used Syncronis C18 column (150 × 4.6 mm with a particle size of 5 µm) connected to quadruple with Time Of Flight (TOF) operated in ESI positive mode at a capillary voltage of 2510 nA. PQ was detected at UV-232 nm followed by mass-spectrometry analysis. The resulting data was analyzed using DataAnalysis 4.2 software from Bruker. PQ was quantified using an MS intensity peak of, 171.092 (Cheng and Hercules 2001), the most abundant ion generated under the above-mentioned conditions. Peak specificity for PQ was confirmed by MS-MS spectra in all the samples. Pure PQ (Sigma, Cat No. 856177) was used to obtain the standard curve for quantification.

Data availability

Supplementary material is available at figshare at https://doi.org/10.25386/genetics.13466588.

Results

DPY-7, DPY-8, DPY-9, and DPY-10 collagens maintain cuticle barrier against exogenous molecules

Aiming to understand the requirement of collagens in the barrier function of *C. elegans* cuticle, we used a standard cuticle permeability assay (Moribe *et al.* 2004). The cuticle serves as a permeability barrier for exogenous molecules such that cell-permeable nucleic acid dye Hoechst 33258 cannot stain nuclei in the head or hypodermis of wild-type *C. elegans*, both lined by a layer of the cuticle (schematic in Figure 1A). We found that wild-type N2 animals do not show staining of nuclei in the head region (Figure 1C) or in the hypodermis (data not shown) in Hoechst stain assay. The loss of glycosyltransferase BUS-8 caused permeability defect and staining of head nuclei in *bus-8(e2698)* animals (Figure 1B) consistent with the previous report (Partridge *et al.* 2008). To test whether collagens regulate Hoechst 33258 permeability, we performed a large-scale RNAi screen against 93 collagen-encoding genes, available in Ahringer RNAi library. As shown in Supplementary Table S1, the majority of collagens tested under the condition of RNAi, appeared dispensable for permeability barrier function in Hoechst 33258 permeability assay. However, we found that 4 cuticular collagens, DPY-7, DPY-8, DPY-9, and DPY-10, were required to maintain the barrier and showed staining of head nuclei with Hoechst 33258 upon RNAi (Figure 1, D–G). We termed them PD collagens. PD collagen mutants-*dpy-7(e88)*, *dpy-8(e1281)*, *dpy-9(e12)*, and *dpy-10(e128)*—also had permeability defect (Supplementary Figure S1).

Since all PD collagens also cause Dpy phenotype in *C. elegans*, we tested whether dumpy phenotype was responsible for permeability to Hoechst stain. We tested two cuticular collagens with known Dpy phenotype, DPY-4, and DPY-5, for the permeability barrier function. *dpy-4* and *dpy-5* RNAi animals showed dumpy phenotype like PD collagens (data not shown) but no Hoechst

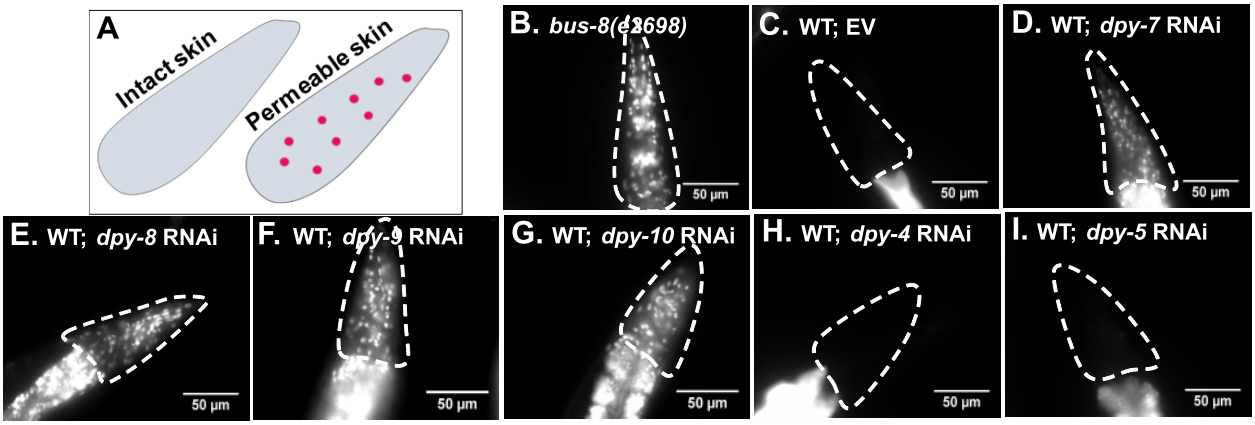

Figure 1 Four collagens encoded in *C. elegans* genome maintain cuticle barrier function. (A) Pictorial representation of Hoechst staining in *C. elegans*. Hoechst 33258 staining-based permeability assay of (B) *bus-8(e2698)* and (C) EV, (D) *dpy-7*, (E) *dpy-8*, (F) *dpy-9*, (G) *dpy-10*, (H) *dpy-4*, and (I) *dpy-5* RNAi animals. Scale bar, 50 µm. $n = 3$; $N \geq 15$.

permeability defect (Figure 1, H and I). This suggested that Dpy phenotype is not linked to permeability defect. Taken together, our analysis uncovered the function of 4 specific collagens as molecular determinants of cuticle permeability barrier against exogenous molecules in *C. elegans*.

PD collagens maintain the ultrastructure of *C. elegans* cuticle

To understand the nature of permeability defect in PD collagen mutants, we studied structural topography of the cuticle, by confocal microscopy and by scanning electron microscopy. For confocal microscopy, we studied the spatial localization of COL-19, adult-specific collagen localized to annuli, and alae in the cuticle of WT animals (Supplementary Figure S3A) (Thein *et al.* 2003). Annuli are thick areas of the cuticle separated by furrows while alae are longitudinal ridges that join ventral and dorsal cuticle in *C. elegans* (Page and Johnstone 2007). In control animals, COL-19::GFP containing annuli were arranged in a parallel and periodic manner, orthogonal to alae (Supplementary Figure S3A). Knockdown of *dpy-7*, *dpy-8*, *dpy-9*, *and dpy-10* altered COL-19::GFP expression in the cuticle (Supplementary Figure S3, D–G), also reported recently for *dpy-7* and *dpy-10* (Dodd *et al.* 2018). In PD collagen RNAi animals, COL-19 spatial expression was altered such that annuli containing COL-19::GFP appeared thicker, irregular, and non-parallel (Supplementary Figure S3, D–G). This suggested that PD collagens knockdown either (a) causes incorrect positioning of COL-19 *per se* in the cuticle, or (b) causes cuticular disorganization such that annuli and furrows themselves are not arranged properly. To distinguish between these two possibilities, we performed high-resolution scanning electron microscopy at 50,000× magnification. Using SEM, we found that in WT animal's cuticle showed a regular and periodic arrangement of annuli separated by furrows (Figure 2A and Supplementary Figure S2A) as shown earlier (Cox *et al.* 1981b). Although *dpy-7*, *dpy-8*, and *dpy-10* mutants were described as smooth and lacking annular furrows (McMahon *et al.* 2003), we could visualize furrow-like indentations using high-resolution SEM imaging. In PD collagen mutant animals, we observed discontinuous and non-parallel indentations (Figure 2, D–G and Supplementary Figure S2, D–F).

It was interesting to note that RNAi of *dpy-4* and *dpy-5* altered COL-19::GFP expression near alae region (a feature qualitatively different from *dpy-7*, *dpy-8*, and *dpy-10* RNAi) but *dpy-4* and *dpy-5* RNAi animals showed periodic organization of annuli in regions distal to alae (Supplementary Figure S3, B and C) as shown earlier (Dodd *et al.* 2018). SEM study of *dpy-4* and *dpy-5* animals showed normal ultrastructure of the cuticle (Figure 2, B and C and Supplementary Figure S2, B and C) similar to control animals. Both *dpy-4* and *dpy-5* RNAi animals had a periodic arrangement of annuli and furrows, and they lacked irregular indentations visible in *dpy-7*, *-8*, and *-10* RNAi animals. This suggested again that Dpy phenotype *per se* is not linked to either the barrier function defect of the cuticle or to ultra-structural defects in the cuticle. Taken together, our analyses of permeability barrier function and of cuticle ultrastructure in collagen deficient animals indicate that defects in the cuticle originating from lack or reduced function of PD collagen increase permeability of *C. elegans* cuticle to exogenous molecules.

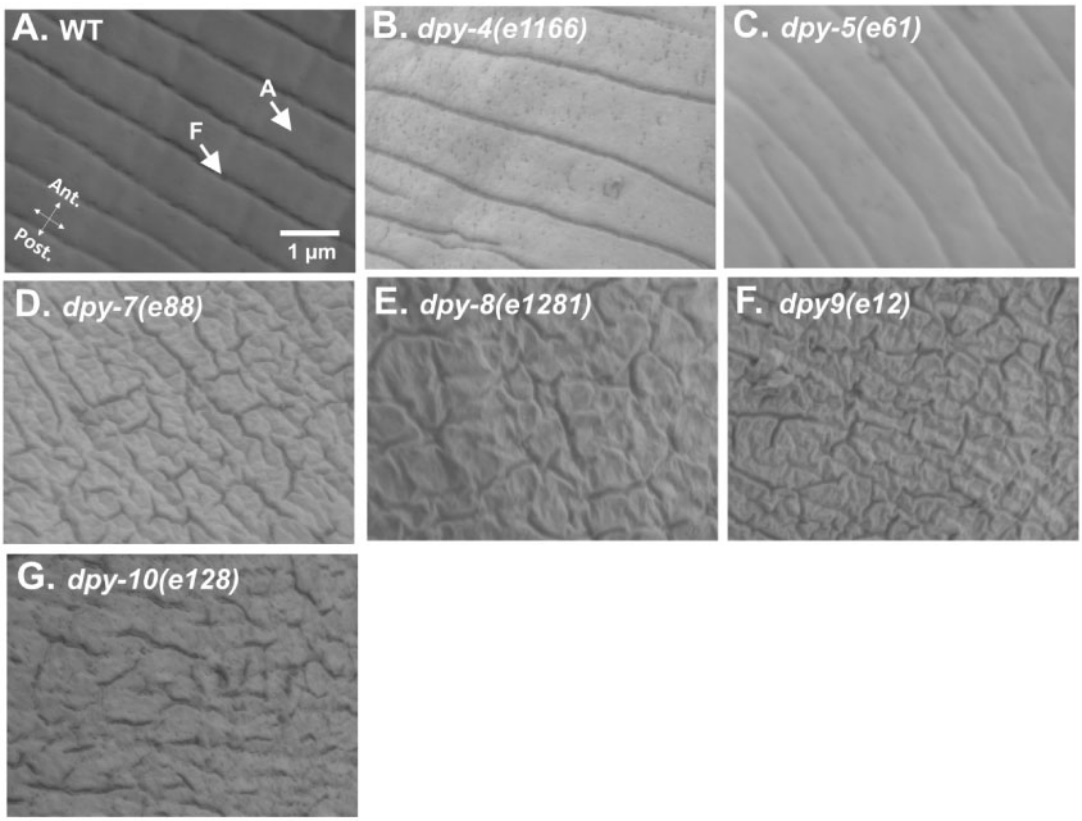

Figure 2 PD collagens maintain the ultra-structure of *C. elegans* cuticle. Scanning electron micrograph of (A) WT, (B) *dpy-4(e1166)*, (C) *dpy-5(e61)*, (D) *dpy-7(e88)*, (E) *dpy-8(e1281)*, (F) *dpy-9(e12)*, and (G) *dpy-10(e128)* animals (50,000× magnification). Annuli, *A*, furrows, *F*, anterior, Ant, and posterior, Post., of the worms are indicated. Scale bar, 1 µm.

PD collagens protect *C. elegans* on paraquat, levamisole, and ivermectin

Skin provides a large surface area for diffusion of a variety of environmental toxins into the body. We hypothesized that reduced function of PD collagens can cause rapid infiltration of exogenous molecules in *C. elegans* habitat and can lead to reduced survival of *C. elegans* against environmental toxins. To test this, we checked the survival of WT and PD collagens deficient animals on methyl viologen dichloride hydrate or paraquat, a herbicide abundantly present in farmland soil. We found that mutations in either of the four PD collagens—*dpy-7(e88)*, *dpy-8(e1281)*, *dpy-9(e12)*, and *dpy-10(e128)*—caused enhanced susceptibility to 20 mM PQ, compared to WT animals (Figure 3, A and B). RNAi for *dpy-7*, *-8*, *-9*, *and -10* could phenocopy the Dpy phenotype (data

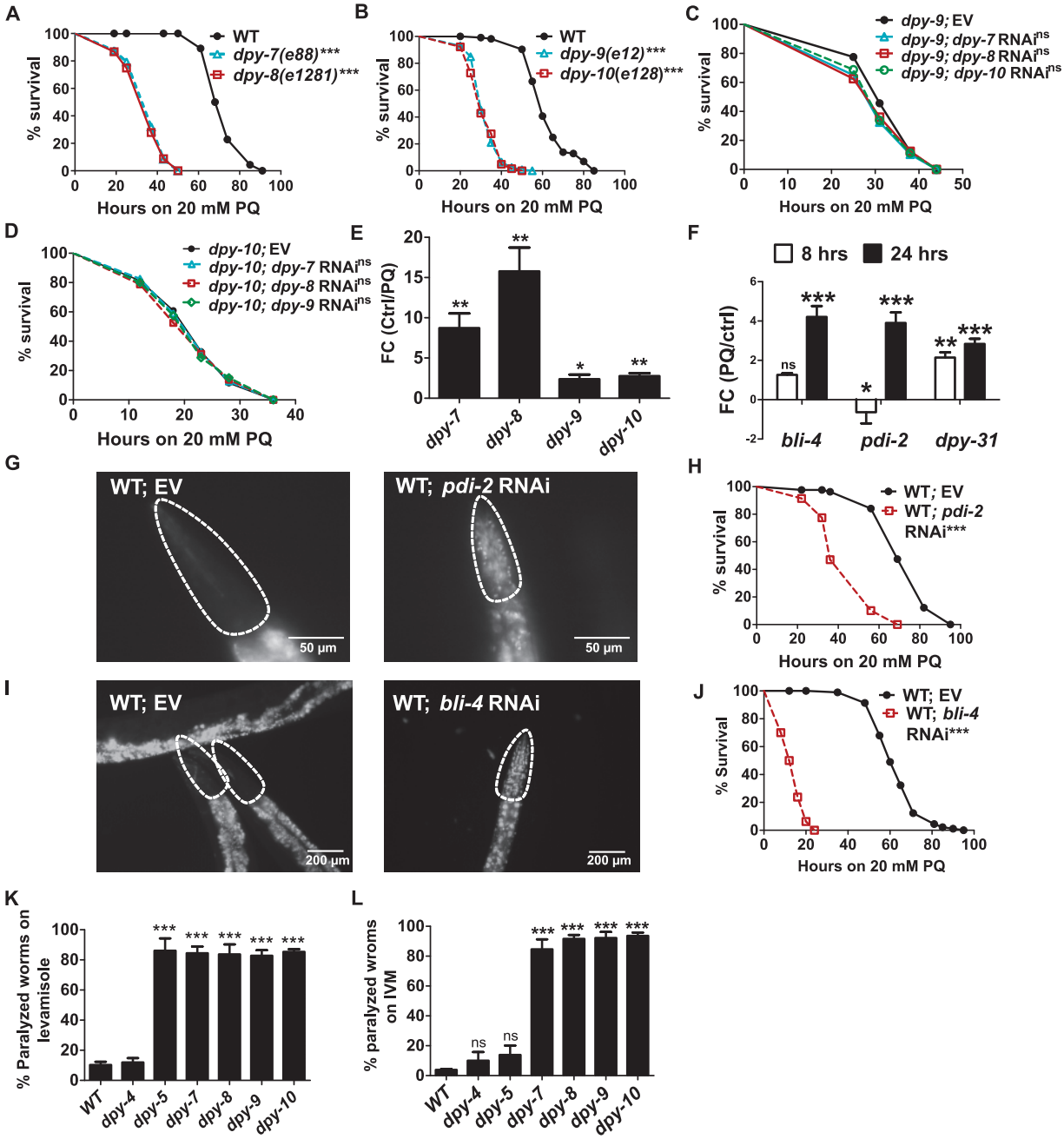

Figure 3 PD collagens positively regulate survival of *C. elegans* on exogenous toxins. Kaplan–Meier survival curves of (A) WT, *dpy-7(e88)* and *dpy-8(e1281)* animals on 20 mM paraquat (PQ), (B) WT, *dpy-9(e12)* and *dpy-10(e128)* animals on 20 mM PQ, (C) *dpy-9(e12)* animals with RNAi of EV, *dpy-7*, *dpy-8* and *dpy-10* on 20 mM PQ, (D) *dpy-10(e128)* animals with RNAi of EV, *dpy-7*, *dpy-8* and *dpy-9* on 20 mM PQ. $n = 3$; $N \geq 50$ for panels A–D. (E) qRT-PCR analysis of PD collagens in WT animals exposed to 20 mM PQ for 8 h. (F) qRT-PCR analysis of collagen processing enzymes in WT animals exposed to 20 mM PQ for 8 and 24 h. (G) Hoechst 33258 staining in WT animals with EV and *pdi-2* RNAi. $n = 2$; $N \geq 15$. Kaplan–Meier survival curves of WT animals with (H) EV and *pdi-2* RNAi animals on 20 mM PQ. $n = 3$; $N \geq 50$. (I) Hoechst 33258 staining in WT animals with EV and *bli-4* RNAi. $n = 2$; $N = 15$. Kaplan–Meier survival curves of WT animals with (J) EV and *bli-4* RNAi animals on 20 mM PQ. $n = 3$; $N \geq 40$. Percent paralyzed of WT, *dpy-4(e1166)*, *dpy-5(e61)*, *dpy-7(e88)*, *dpy-8(e1281)*, *dpy-9(e12)*, and *dpy-10(e128)* animals upon (K) exposure to 125 µM levamisole and, (L) 50 µM Ivermectin (IVM). $n = 3$; $N \geq 40$ for panels K and L. Error bars indicate SEM. $n = 3$; $N \geq 50$. $^*P \leq 0.05$, $^{**}P \leq 0.005$, $^{***}P \leq 0.0005$, NS—not significant, for Student's *t*-test and Mantel–Cox test for survival curves. *P*-value for survival curves are indicated next to genotypes. For TD^{50} values in survival assays, see Supplementary Table S2.

not shown) as well as caused enhanced PQ susceptibility compared to control (Supplementary Figure S4, A and B). *dpy-7(e88)*, *dpy-8(e1281)*, *dpy-9(e12)*, and *dpy-10(e128)* animals were also susceptible to low dose (2 mM) PQ (Supplementary Figure S4, C and D) which had a very mild effect on WT animals. To understand whether PD collagens had a non-redundant or overlapping function in survival against PQ, we tested the effect of PD collagen RNAi in PD collagen mutants. RNAi of *dpy-7*, *-8*, or *-10* did not cause any increase in PQ susceptibility of *dpy-9(e12)* animals (Figure 3C). Similarly, RNAi of *dpy-7*, *-8*, or *-9* did not cause any increase in PQ susceptibility of *dpy-10(e128)* animals (Figure 3D). Consistent with the lack of Hoechst 33258 permeability defect in *dpy-4* and *dpy-5* animals, RNAi of *dpy-4* and *dpy-5* did not affect their survival on PQ (Supplementary Figure S4E). Despite enhanced susceptibility to PQ, *dpy-7(e88)*, *dpy-8(e1281)*, *dpy-9(e12)*, and *dpy-10(e128)* animals showed resistance to intestinal infection by *P. aeruginosa* PA14 (Supplementary Figure S4, F and G) consistent with reports of their resistance to skin invasion by pathogenic fungus *D. coniospora* (Pujol *et al.* 2008b; Zugasti *et al.* 2014; Dodd *et al.* 2018) as well-increased expression of some lectins and caenacins linked to immune response (Rohlfing *et al.* 2010). These animals also showed enhanced resistance to osmotic stress (Supplementary Figure S4J) as reported earlier (Lamitina *et al.* 2006; Wheeler and Thomas 2006). We also tested *dpy-9* and *dpy-10* mutants (Supplementary Figure S4H) and *dpy-7* and *dpy-8* RNAi animals (Supplementary Figure S4I) for heat stress susceptibility and found that these animals had enhanced resistance to thermal stress at 32°C compared to control. *dpy-7* and *dpy-8* RNAi animals also exhibited enhanced resistance to osmotic stress (Supplementary Figure S4I). In all, the study of survival under different stresses indicated that PD collagens negatively regulate *C. elegans* response to heat stress and osmotic stress, but they are essential for survival against exogenous paraquat.

We asked if PQ causes damage to the cuticle. To test this, we checked permeability of cuticle in WT animals upon exposure to PQ. We found an increase in the cuticle permeability upon exposure to PQ for as early as 12 h (Supplementary Figure S5). If collagens are essential for survival on PQ, PD collagen transcription might be elevated during PQ exposure to repair the damage caused by PQ. Therefore, we examined the levels of transcripts of PD collagens in WT animals upon PQ exposure and found that transcripts were upregulated 2.5- to 15-fold, compared to untreated animals (Figure 3E). Collagen processing enzymes are required for proper folding, processing, and secretion of collagens (schematic in Supplementary Figure S4K). PDI-2, an endoplasmic reticulum protein disulfide isomerase, is essential for oxidative folding of protocollagen strands (Winter *et al.* 2007), BLI-4 is a serine endoprotease which is required for N-terminal processing (Winter *et al.* 2007), and DPY-31 is a metalloprotease required for C-terminal processing of collagens (Stepek *et al.* 2010). We found that transcripts for *pdi-2*, *bli-4*, and *dpy-31* were significantly upregulated at 24 h of PQ exposure while the transcript for *dpy-31* was upregulated even at 8 h of PQ exposure (Figure 3F) compared to untreated control. In addition, RNAi of *pdi-2* and *bli-4* increased permeability of WT animals to Hoechst 33258 stain (Figure 3, G–I) and led to enhanced susceptibility to PQ-induced death (Figure 3, H–J). We also tested *dpy-31* RNAi but we did not see neither Dpy phenotype (reported by Novelli *et al.* 2004) nor enhanced permeability (data not shown). Altogether, these data suggest that collagen processing enzymes support the survival of *C. elegans* against PQ likely by promoting proper folding, processing, and secretion of collagens.

To test if PD collagens provide broad protection from exogenous toxins, we tested toxins which do not cause oxidative stress. We tested the effect of two anthelminthic drugs—levamisole and ivermectin—on *C. elegans*. Both drugs act at the neuromuscular junction and cause paralysis in worms (Kass *et al.* 1980; Lewis *et al.* 1980; Atchison *et al.* 1992; Fay, 2005–2018). We found that all four PD collagen mutants had severe susceptibility to drug-induced paralysis within minutes of exposure, compared to WT control (Figure 3, K and L). We also tested *dpy-4(e1166)* and *dpy-5(e61)* for paralysis on levamisole and ivermectin. *dpy-5(e61)* animals showed paralysis comparable to WT animals on both levamisole and ivermectin (Figure 3, K and L). Interestingly, *dpy-4(e1166)* animals showed faster paralysis on levamisole but not on ivermectin exposure (Figure 3, K and L). This suggested that collagen requirement in permeability barrier maintenance varies with structure and size of the molecule. Taken together, these results show that permeability barrier maintenance by PD collagens is necessary for the protection of *C. elegans* against exogenous toxins.

DPY-7, DPY-8, DPY-9, and DPY-10 belong to the group of collagens which causes furrow defect. Two other collagens, DPY-2 and DPY-3 are also shown to cause furrow defect similar to PD collagens (Dodd *et al.* 2018). We tested if these collagens are also required for maintaining cuticle barrier function. We found that *dpy-2* and *dpy-3* RNAi increased cuticle permeability to Hoechst stain (Supplementary Figure S6A) and enhanced susceptibility to PQ, levamisole, and ivermectin (Supplementary Figure S6, B–D). This suggests that collagens required to lay down the furrows are important for permeability barrier function of the cuticle and survival against exogenous toxins.

dpy-9 and dpy-10 animals incur accelerated tissue damage and increased influx of toxin during paraquat exposure

Enhanced susceptibility of PD collagen deficient animals to PQ-induced death prompted us to hypothesize that these animals incur greater damage during PQ exposure. PQ-induced damage is due to ROS production (Gage 1968; Bus *et al.* 1976; Bus and Gibson 1984). ROS damage can be countered by boosting cellular glutathione production via N-acetylcysteine (NAC) supplementation (Thor *et al.* 1979; Oh *et al.* 2015) as seen in WT animals (Figure 4, A and B). However, supplementation of NAC did not enhance the survival of *dpy-9(e12)* (Figure 4A) or of *dpy-10(e128)* (Figure 4B) animals against PQ stress. This data suggested that antioxidants insufficiency was not responsible for the susceptibility of *dpy-9* and *dpy-10* animals. It raised the possibility that *dpy-9* and *dpy-10* animals may incur tissue damage in such an accelerated manner that the damage could not be contained by NAC supplementation. If this was true, organ function should decline faster in Dpy animals. We tested this by assaying the muscular function of the pharyngeal grinder during exposure to PQ. We found that the pharyngeal pumping rate declined dramatically (by 95%) in *dpy-9* and *dpy-10* mutants upon 12-h exposure to PQ compared to only 25% decline in WT animals (Figure 4C) indicating rapid loss of tissue function in PD collagen animals.

Accelerated tissue damage could happen due to the rapid influx of PQ. To test this possibility, we quantified the accumulation of PQ in whole worm lysate, by liquid chromatography followed by mass spectrometry (LC-MS/MS). Upon 12-h exposure to PQ, both *dpy-9* and *dpy-10* RNAi animals had significantly higher PQ per animal than EV animals (Figure 4, D and E) indicating that the influx of paraquat was indeed much higher in Dpy animals than in WT. Increased accumulation of PQ in Dpy

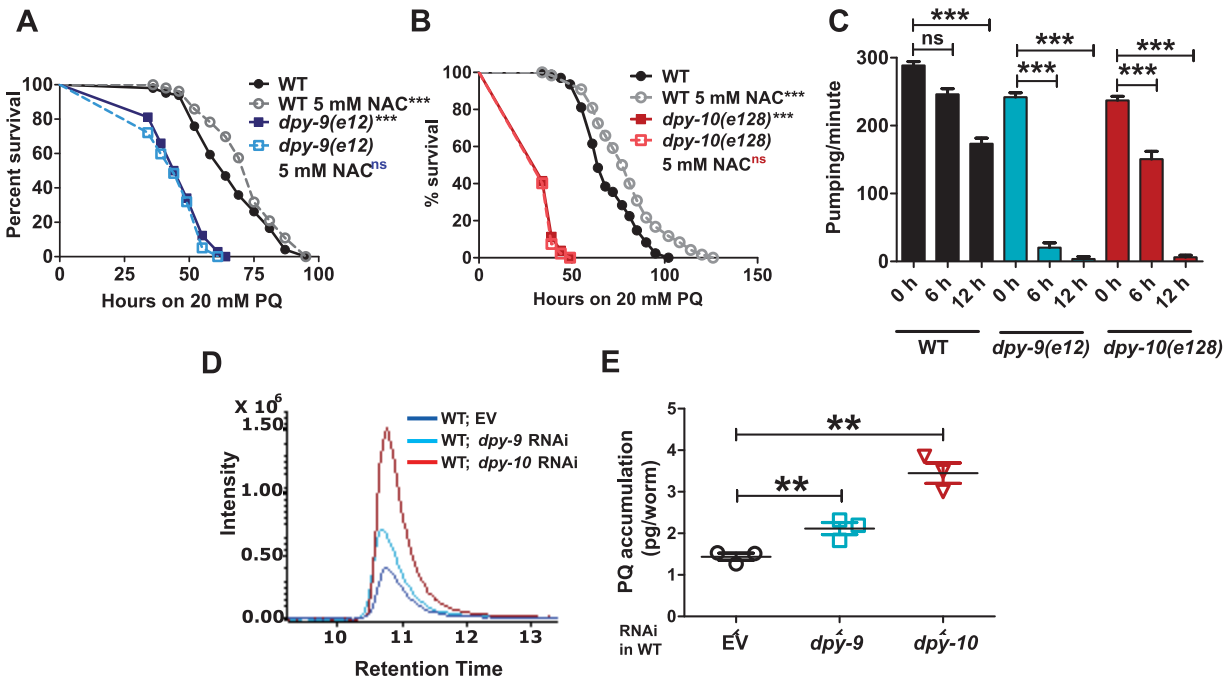

Figure 4 PD collagen mutants show enhanced accumulation of PQ and increased damage during PQ exposure. Kaplan–Meier survival curves of (A) EV and *dpy*-9 RNAi animals treated with or without 5 mM NAC, on 20 mM PQ, (B) of EV and *dpy*-10 RNAi animals treated with or without 5 mM NAC, on 20 mM PQ. $n = 3$; $N \geq 50$ for panels A and B. (C) Pharyngeal pumping rate in WT, *dpy*-9 *(e12)*, and *dpy*-10 *(e128)* animals upon exposure to 20 mM PQ for 0, 6, and 12 h. $n = 3$; $N \geq 10$. (D) LC-MS/MS analysis of PQ accumulation in EV, *dpy*-9, and *dpy*-10 RNAi animals upon exposure to 20 mM PQ for 12 h. (E) Quantification of PQ accumulation per animal. Error bars indicate SEM. *, $P \leq 0.05$; **, $P \leq 0.005$; ***, $P \leq 0.0005$; NS—not significant, $P \geq 0.05$, significance based on Student's *t*-test and Mantel–Cox test for survival curves. *P*-value for survival curves are indicated next to genotypes. For TD^{50} values in survival assays, see Supplementary Table S2.

animals is consistent with increased permeability in PD collagen animals. Taken together, the data suggested that enhanced susceptibility of *dpy*-9 and *dpy*-10 animals to PQ is due to increased toxin accumulation and accelerated tissue damage.

dpy-9 and *dpy*-10 mutants show robust oxidative stress response upon PQ exposure

Free radicals generated during oxidative stress can damage proteins, lipids, and other biomolecules. Antioxidants play a crucial role in the defense against oxidative damage via the production of glutathione S-transferases (GSTs), glutathione peroxidase (GPXs), superoxide dismutases (SODs), and catalases (CTLs) in response to oxidative stress (Birben *et al.* 2012). We tested if the enhanced susceptibility of PD collagen deficient animals toward PQ resulted from an altered transcription of genes for antioxidants in the mutants. We examined the transcript level of 19 genes from 4 families of antioxidants reported to be up-regulated under oxidative stress (Park *et al.* 2009). Of the 19 transcripts examined, eleven were induced in WT animals as well as in *dpy*-9*(e12)* and *dpy*-10*(e128)* animals upon exposure to PQ (Table 1). *dpy*-9*(e12)* and *dpy*-10*(e128)* animals showed induction of 7 additional antioxidant genes beyond the inducibility observed in WT animals (Figure 5A and Table 1). Transcripts for *gst*-4, *gst*-12, and *gst*-30 were induced many folds by PQ in all genetic backgrounds (Table 1). For confirmation, we also utilized a *gst*-4*p*::GFP reporter strain. We found that P*gst*-4::GFP was induced equally well in EV control and *dpy*-10 RNAi animals upon exposure to PQ for 6 h (Figure 5B, also see Table 1) or in *dpy*-9 RNAi animals upon paraquat exposure (Supplementary Figure S7). Interestingly, *dpy*-9*(e12)* and *dpy*-10*(e128)* animals also showed high basal level of many antioxidants (Supplementary Figure S8, A–D). Altogether, the data showed that antioxidants machinery is intact and functional in *dpy*-9 and *dpy*-10 mutants, suggesting that permeability defects of PD collagen deficient animals contribute to their enhanced susceptibility to PQ.

Transcription factor BLMP-1 maintains the permeability barrier of *C. elegans* cuticle and PD collagen expression

In *C. elegans*, cuticular collagen expression is controlled exquisitely to allow molting during larval development as well as during dauer formation. However, the identity of the transcription factor(s) involved in permeability barrier maintenance is not known. In ChIP-seq study by Niu *et al.* (2011), the BLMP-1 transcription factor had peaks in PD collagen genes although another study by Hyun *et al.* (2016) suggested BLMP-1 could be a negative regulator of certain collagens not including PD collagens. We first tested if BLMP-1 is required for maintaining permeability. RNAi of *blmp*-1 caused permeability barrier defect and staining of nuclei by Hoechst 33258 (Figure 6, A and B). Consistent with the permeability defect, *blmp*-1 RNAi animals also showed enhanced susceptibility to PQ (Figure 6C). To test if BLMP-1 regulates permeability via its regulation of transcription of collagens, we first examined the effect of *blmp*-1 RNAi on COL-19::GFP expression. COL-19::GFP expression was diminished in *blmp*-1 RNAi animals (Supplementary Figure S9, A–C). We also examined level of transcripts for PD collagens in *blmp*-1 RNAi animals by qRT PCR (Figure 6D). We found that expression of PD collagens along with *dpy*-4 and *dpy*-5 was reduced in *blmp*-1 RNAi animals. We found that expression of *dpy*-2 and *dpy*-3 was also significantly reduced in *blmp*-1 RNAi animals (Supplementary Figure S6E). We also observed reduction in expression level of collagens

Table 1 Antioxidant genes expression in WT, *dpy-9(e12)*, and *dpy-10(e128)* animals upon 20 mM PQ exposure

Genes	WT PQ/ctrl		*dpy-9(e12)* PQ/ctrl		*dpy-10(e128)* PQ/ctrl	
	Fold change (Mean[a] ± SEM)	*P*-value	Fold change (Mean[a] ± SEM)	*P*-value	Fold change (Mean[a] ± SEM)	*P*-value
sod-1	1.7 ± 0.2	*	3.2 ± 0.5	*	3.5 ± 0.7	*
sod-2	1.3 ± 0.1	*	0.5 ± 0.8	NS	1.3 ± 0.2	NS
sod-3	0.1 ± 0.9	NS	1.9 ± 0.3	NS	3.3 ± 0.5	*
sod-4	1.6 ± 0.1	**	4.7 ± 0.3	***	3.7 ± 0.4	**
sod-5	1.6 ± 0.3	NS	2.7 ± 0.5	*	15.8 ± 4.4	*
gcs-1	1.6 ± 0.1	**	5.1 ± 0.5	**	3.5 ± 0.4	**
gst-4	5.9 ± 0.7	***	18.4 ± 2.9	**	5.5 ± 0.4	**
gst-12	5.1 ± 1.2	*	31.7 ± 2.6	***	7.3 ± 1.6	**
gst-30	16.9 ± 1.6	**	130.9 ± 11.7	***	61.8 ± 12.0	***
ctl-1	2.6 ± 0.2	***	2.7 ± 0.2	***	2.3 ± 0.4	***
ctl-2	2.3 ± 00	***	2.4 ± 0.0	***	2.8 ± 0.1	**
gpx-1	0.6 ± 1.2	NS	2.9 ± 0.1	*	1.7 ± 0.1	***
gpx-2	1.9 ± 0.2	*	2.5 ± 0.4	***	2.4 ± 0.1	
gpx-3	−0.5 ± 0.8	NS	−1.8 ± 0.1	***	0.6 ± 1	NS
gpx-4	0.3 ± 0.7	NS	1.6 ± 0.1	***	1.4 ± 0.1	NS
gpx-5	−1.9 ± 1.9	NS	−1.1 ± 0.0	*	3.0 ± 0.3	**
gpx-6	1.8 ± 0.2	*	4.8 ± 0.9	*	2.4 ± 0.2	**
gpx-7	1.9 ± 0.3	*	2.2 ± 0.3	*	1.9 ± 0.2	*
gpx-8	1.9 ± 0.4	NS	1.6 ± 0.1	*	1.6 ± 0.1	*

NS, not significant, Student's t-test.
[a] Fold change.
* $P \leq 0.05$,
** $P \leq 0.005$,
*** $P \leq 0.0005$.

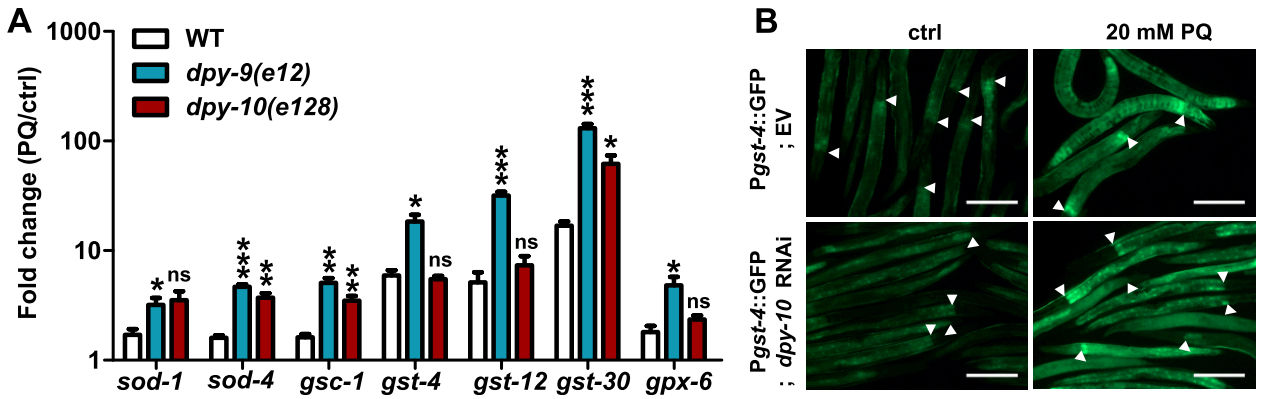

Figure 5 *dpy*-9 and *dpy*-10 mutants display robust oxidative stress response. (A) Comparison of inducibility of detoxification genes in WT, *dpy*-9 *(e12)*, and *dpy*-10 *(e128)* animals upon exposure to 20 mM PQ compared to untreated animals for 6 animals upon exposure to e SEM. Significance is provided for comparisons between inducibility observed in mutants over WT. (B) *gst*-4p::GFP induction in EV and *dpy*-10 RNAi animals upon exposure to 20 mM PQ for 6 h. Arrow heads indicate pharynx and intestine junction. In addition, see Table 1 for inducibility of genes due to PQ exposure. *, $P \leq 0.05$; **, $P \leq 0.005$; ***, $P \leq 0.0005$; NS—not significant, significance based on Student's t-test.

processing enzyme *pdi-2* upon *blmp-1* RNAi. *dpy-31* and *bli-4* expression remained unaltered in *blmp-1* RNAi animals. Altogether, these experiments show that BLMP-1 positively regulates PD collagens expression, permeability barrier maintenance, and protection of worms from PQ.

Intact permeability barrier, as well as antioxidant responses, is essential for the survival of *C. elegans* on paraquat

Several genetic pathways including those regulated by SKN-1, DAF-16, ELT-3, SMK-1 have been shown to regulate *C. elegans* oxidative stress response (An and Blackwell 2003; Wolff *et al.* 2006; Rodriguez *et al.* 2013; Hu *et al.* 2017; Wu *et al.* 2017). *daf-2* encodes an insulin-like growth factor receptor and loss of *daf-2* function provides enhanced resistance to oxidative stress due to higher basal levels of anti-oxidant enzymes (Honda and Honda 1999; Tullet *et al.* 2008) and resistance to thermal stress, attributed to elevated levels of heat shock proteins (Lithgow *et al.* 1995; Hsu *et al.* 2003). If increased PQ accumulation and ensuing damage were a major contributor to death as our data suggests, disrupting the permeability barrier in *daf-2(e1370)* should make them susceptible to PQ despite enhanced antioxidant defenses of the mutant animals. RNAi of *dpy-7*, *dpy-8*, and *dpy-10* was effective in *daf-2(e1370)* animals and caused significant Dpy phenotype (Supplementary Figure S10, A–D). Also, RNAi of *dpy-7*, *dpy-8*, and *dpy-10* significantly increased the cuticle permeability of *daf-2(e1370)* animals to Hoechst 33258 stain (Figure 7, A–D). Importantly, RNAi of PD collagens in *daf-2(e1370)* animals suppressed enhanced PQ resistance (Figure 7, E–G) but further enhanced the thermal resistance (Supplementary Figure S10, E–G) indicating that thermal stress resistance and PQ resistance responses are not linked. In all, the data suggested that intact permeability barrier of the cuticle is essential for survival of *daf-2* animals on exogenous toxin paraquat but not for thermal stress resistance.

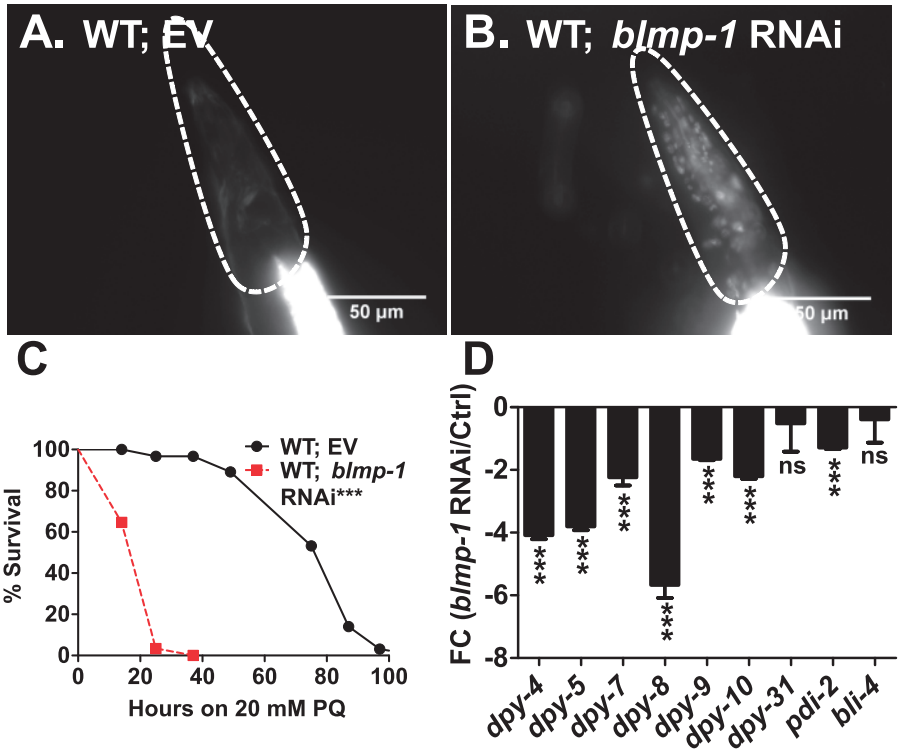

Figure 6 Transcription factor BLMP-1 regulates cuticle permeability and survival of worms on PQ. Hoechst 33258 permeability assay in (A) EV and (B) *blmp-1* RNAi in WT animals. Scale bar, 50 µm. $n = 3$; $N \geq 15$. Kaplan–Meier survival curves of (C) EV control and *blmp-1* RNAi animals against 20 mM PQ. $n = 3$; $N \geq 50$. qRT-PCR analysis of transcripts for collagens and collagen processing enzymes upon (D) *blmp-1* RNAi *in* WT animals compared to EV control. Error bars indicate SEM. *, $P \leq 0.05$; **, $P \leq 0.005$; ***, $P \leq 0.0005$; NS—not significant, $P \geq 0.05$, significance based on Student's *t*-test and Mantel–Cox test for survival curves. *P*-value for survival curves are indicated next to genotypes. For TD^{50} values in survival assays, see Supplementary Table S2.

Enhanced oxidative stress resistance of *daf-2* animals is dependent on the forkhead box O transcription factor, DAF-16 (Honda and Honda 1999). We asked if DAF-16 was required for maintenance of the cuticle barrier function, for induction of the antioxidant defenses, or both. We examined the cuticle structure of *daf-2(e1370)* animals and found it to be similar to WT animals (Figure 7H). *dpy-10* RNAi caused ultra-structural defects in *daf-2(e1370)* animals (Figure 7I), but RNAi inhibition of *daf-16* did not alter the ultrastructure of cuticle in either WT animals (Figure 7K) or in *daf-2(e1370)* animals (Figure 7J). *daf-16* RNAi animals showed parallel, equidistant furrows in WT as well as *daf-2(e1370)* animals comparable to respective EV controls. *daf-16* RNAi suppressed the enhanced oxidative stress resistance of *daf-2(e1370)* animals on PQ (Figure 7L) as shown earlier (Honda and Honda 1999), but did not affect Hoechst 33258 permeability in *daf-2(e1370)* or WT animals (Figure 7, N and O). Interestingly, while *daf-16* RNAi suppressed the enhanced thermal stress resistance of *daf-2(e1370)* animals, *dpy-10* RNAi further enhanced the survival of *daf-2(e1370)* animals against thermal stress (Figure 7M). Based on these results, we inferred that DAF-16 promoted survival on PQ by regulating antioxidant responses, while DPY-10 regulated protection by maintaining the barrier function of the cuticle and by preventing damage. To further confirm this, we analyzed transcript levels of antioxidant genes upon RNAi of *daf-16* and *dpy-10* in *daf-2(e1370)* animals. At the basal level, the expression of antioxidants in *daf-2(e1370)* was dependent on DAF-16 but not on DPY-10 (Figure 7P). Four of the six genes tested were inducible by PQ exposure in *daf-2* animals (Figure 7Q). We found that PQ mediated inducibility of antioxidant genes in *daf-2(e1370)* animals was dependent on DAF-16 but not on DPY-10 compared to EV animals (Figure 7R). In fact, transcripts for four of the 6 antioxidants tested were further induced due to *dpy-10* RNAi while *sod-3* was not. Altogether, analyses of the ultrastructure of the cuticle, of survival, and of stress response signatures in *daf-2* animals indicated that survival on PQ requires both an intact permeability barrier and DAF-16 dependent antioxidant machinery.

We propose a model (Figure 7S) to describe the essential function of PD collagens—DPY-2, DPY-3, DPY-7, DPY-8, DPY-9, and DPY-10—in maintaining cuticle ultrastructure and permeability barrier in *C. elegans*. These collagens allow *C. elegans* cuticle to keep exogenous toxins out, thereby preventing rapid damage and death. Transcription factor BLMP-1 regulates expression of collagens and helps maintain the permeability barrier.

Discussion

Skin serves as an interface as well as a barrier between an organism and its environment. In this study, we demonstrate that skin indeed protects *C. elegans* from exogenous toxins and six PD collagens play a protective role, by maintaining the barrier function of the cuticle. We show that loss of DPY-7, DPY-8, DPY-9, and DPY-10—causes ultrastructural defects. Compromised cuticle permeability is associated with increased accumulation of paraquat, greater tissue damage, and accelerated death. Concomitantly, PD collagens, as well as collagen processing enzymes, are upregulated in response to PQ, likely to maintain cuticle integrity. We also show that BLMP-1 transcription factor positively regulates survival on the paraquat and permeability barrier function of the cuticle. Importantly, BLMP-1 regulates the expression of PD collagens. Defect in anyone of the 6 collagens or *blmp-1* causes enhanced susceptibility to exogenous molecules such as levamisole

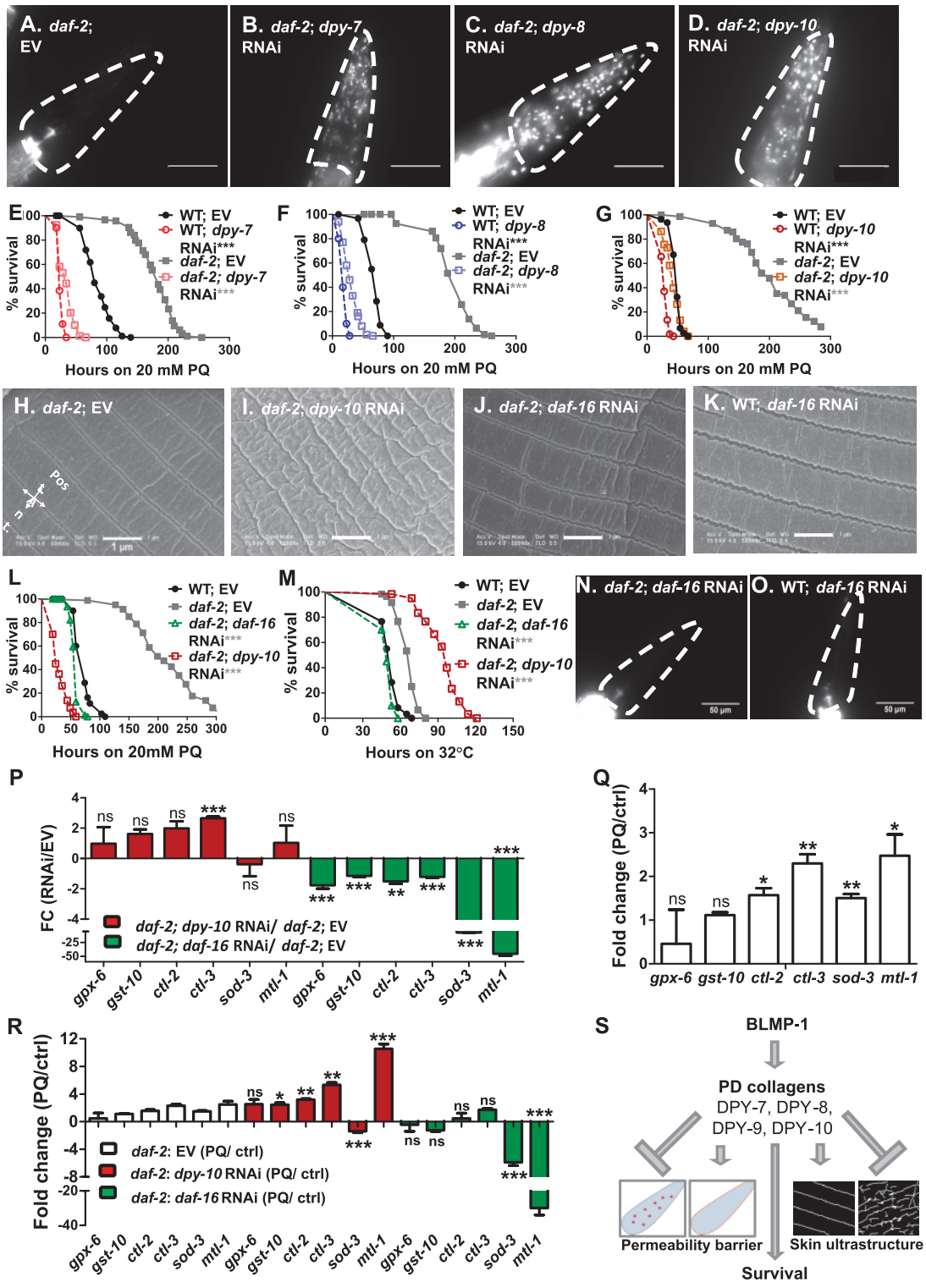

Figure 7 DPY-10 does not affect DAF-16 dependent antioxidants expression in *daf-2* mutant. Hoechst 33258 staining-based permeability assay in (A) EV, (B) *dpy-7*, (C) *dpy-8* and (D) *dpy-10* RNAi in *daf-2 (e1370)* animals. Scale bar, 50 μm. $n = 3$; $N \geq 15$. Kaplan–Meier survival curves of (E) EV and *dpy-7* RNAi, (F) EV and *dpy-8* RNAi, (G) EV and *dpy-10* RNAi treated WT and *daf-2 (e1370)* animals against 20 mM PQ. $n = 3$; $N \geq 50$ for panels E–G. Scanning electron micrographs of (H) EV, (I) *dpy-10 and* (J) *daf-16* RNAi in *daf-2 (e1370)* animals and, (K) *daf-16* RNAi in WT animals at 50,000× magnification. Kaplan–Meier survival curves of EV, *dpy-10 and daf-16* RNAi in *daf-2 (e1370)* animals and, EV RNAi in WT animals against (L) 20 mM paraquat and (M) heat stress at 32°C. $n = 3$; $N \geq 50$ for panels L and M. Hoechst 33258 stained nuclei in (N) *daf-16* RNAi in *daf-2 (e1370)* animals and (O) *daf-16* RNAi in WT animals. Scale bar, 50 μm. $n = 3$; $N \geq 15$ for panels N and O. qRT-PCR analysis of detoxification genes *gpx-6*, *gst-10*, *sod-3*, *ctl-2*, *ctl-3*, and *mtl-1* at (P) basal level in EV, *dpy-10*, and *daf-16* RNAi in *daf-2 (e1370)* animals and (Q) upon 20 mM PQ exposure in *daf-2* animals. (R) Inducibility of detoxification genes in *daf-2 (e1370)* animals with EV, *dpy-10*, and *daf-16* RNAi, exposed to PQ for 6 h over untreated controls. Error bars indicate SEM. *, $P \leq 0.05$; **, $P \leq 0.005$; ***, $P \leq 0.0005$; NS—not significant, $P \geq 0.05$, significance based on Student's *t*-test and Mantel–Cox test for survival curves. *P*-value for survival curves are indicated next to genotypes. Stars in gray color repesent comparision with *daf-2*; EV. For TD^{50} values in survival assays, see Supplementary Table S2. (S) Proposed model for enhanced susceptibility of PD collagen defective animals to exogenous toxins.

and ivermectin. Altogether, this study shows that cuticle barrier maintenance by specific collagens is critical for protection against environmental toxins.

Caenorhabditis elegans genome contains 177 collagen-encoding genes, a majority of these are expressed at some point during development (Cox *et al.* 1984; Cox and Hirsh 1985; Myllyharju and Kivirikko 2004). Although the exact function for the majority of collagens is not known, some redundancy in function is likely. Interestingly, loss of 19 collagen-encoding genes is known to cause phenotypic changes in the body morphology such as roller, dumpy, or blister (Brenner 1974; Cox *et al.* 1980; Kusch and Edgar 1986; Park and Horvitz 1986). This suggests that despite high apparent redundancy some collagens might be unique in their function. Surprisingly, only 6 out of 93 of the tested collagens caused a cuticle barrier function defect. It is possible that we have missed out on one or more PD collagen due to incomplete inhibition in feeding RNAi, the approach we took in our initial screen. Another interesting point to note is that PD collagens are expressed at a lower level than other collagens suggesting that they may not be just the major structural collagen. It is also possible that maintenance of body structure is independent of the barrier function of collagens.

Spatial localization of collagens in the cuticle might determine their role in the structure or function of the cuticle. *dpy-4* and *dpy-5* mutants had regular furrows but altered localization of COL-19 proximal to alae, suggesting that DPY-4 and DPY-5 may have function unrelated to furrow formation. Loss of PD collagens, on the other hand, had disrupted furrow organization all over the cuticle. This raises the possibility that PD collagens regulate furrow formation/organization in the cuticle such that their loss leads to improper annuli formation and larger areas under the furrows. Immunolocalization of DPY-7 and DPY-10 in the furrows of wild-type animals (McMahon *et al.* 2003) provides support for this. Mutations in *dpy-8* or *dpy-10* lead to disruption in the localization of DPY-7 in the furrows suggesting that DPY-8 and DPY-10 may interact with DPY-7 and might be part of furrows themselves. Our SEM study, combined with COL-19::GFP analysis, indicates disruption of furrow organization in *dpy-7*, *dpy-8*, *dpy-9*, and *dpy-10* animals pointing to their role in the regular and periodic organization of furrows. The presence of numerous irregular indentations in the cuticle of 4 PD collagen mutants tested in our study indicates a link between increase in permeability and susceptibility to paraquat and anthelminthic molecules.

Scanning electron microscopy in the ultrahigh-resolution mode allowed us to visualize various features of the cuticle in adult nematodes. The spatial arrangement of furrows was lost in *dpy-7*, *dpy-8*, *dpy-9*, and *dpy-10* RNAi, instead we found indentations somewhat comparable to atomic force microscopy data of few collagen mutants studied earlier (Essmann *et al.* 2017). We found that SEM was also useful in visualizing features of cuticle not accessible by confocal microscopy. For example, alae were reported to be absent in *dpy-5* RNAi animals (Dodd *et al.* 2018) assayed by COL-19::GFP expression. We also could not observe alae using COL-19::GFP reporter, but we could easily visualize alae in *dpy-4* as well as *dpy-5* RNAi animals by SEM (Supplementary Figure S3, H and I). Going forward, high-resolution SEM and AFM approach could be utilized to study structural changes in *C. elegans* cuticle during development, aging, and injury.

Permeability defect could arise from a deficiency in collagens or processing enzymes expression (this study, Schultz *et al.* 2014) or from defect in glycosylation as in *bus* mutants (Partridge *et al.* 2008) or Acyl-CoA Synthetase mutation (Kage-Nakadai *et al.* 2010). TGF-beta signaling pathway and transcription factors such as HSF-1, ELT-1, ELT-3, and SKN-1 have been shown to influence the expression of collagens (Fernando *et al.* 2011; Ewald *et al.* 2015; Yin *et al.* 2015; Brunquell *et al.* 2016; Madaan *et al.* 2018). TGF-beta pathway has been studied extensively in the context of body size regulation and collagen expression regulation (Wang *et al.* 2002; Fernando *et al.* 2011; Yin *et al.* 2015; Savage-Dunn and Padgett 2017; Madaan *et al.* 2018). We assessed transcription factors—SKN-1, HSF-1, ELT-3, and SMA-9 for permeability defect in Hoechst 33258 staining assay. However, we did not find permeability defects in animals with RNAi of any of these transcription factors (data not shown) suggesting that these do not regulate PD collagen expression. BLMP-1, PRDM-1 homolog, has been shown to play an important role in development and stress in *C. elegans* (Niu *et al.* 2011; Hyun *et al.* 2016) including negative regulation of certain collagens, however, its role in the upregulation of cuticle components was not explored. In this study, we showed that BLMP-1 positively regulates the expression of PD collagens and *pdi-2* collagen processing enzyme. Although our analysis was done in the L3 larval stage, regulation of PD collagen in our study is consistent with BLMP-1 peaks in *dpy-7*, *-8*, *-9*, and *-10* in L1 larva stage in the CHIPseq dataset (Niu *et al.* 2011). Also, consistent with absence of BLMP-1 binding peaks in *dpy-31* and *bli-4* promoter, *blmp-1* RNAi did not affect expression of *dpy-31* and *bli-4*. We found that *blmp-1* RNAi did not affect *fat-1* or *dgat-2*, enzymes involved in lipid metabolism, expression suggesting specificity in BLMP-1 regulation of collagens. This would also suggest that *C. elegans* utilizes a set of transcription factors for expression of different collagens and processing enzymes, perhaps in a context-specific (development, stress, infection, etc.) manner. PD collagens themselves show context-dependent effects on *C. elegans* stress response. Knockdown of PD collagens improved survival of *C. elegans* against osmotic stress, thermal stress, and *P. aeruginosa* infection while it caused susceptibility to PQ and antihelminthic drugs.

An interesting question to ask is whether the permeability is dependent on porosity alone or chemical properties of the exogenous molecules also. To understand this, we utilized molecules varying in size from 240 Da to 875 Da as well as their solubility in water. Hoechst stain 33258 is a water soluble (42.5 mg/ml) Bis-benzimides with molecular weight of 533 Da. Ivermectin is macrocyclic lactone with a molecular weight of 875 Da and poor solubility in water (4 µg/ml). Paraquat dichloride is a water soluble (700 mg/ml) organic chloride salt of 4,4′-bipyridine with a molecular weight of 257 Da. Levamisole (Tetramisole hydrochloride) belongs to imidazothiazoles group of organic polycyclic compounds. It has a molecular weight of 240 Da and water solubility of 210 mg/ml. Thus, levamisole has molecular size smaller than Hoechst stain, ivermectin, and PQ. Dodd *et al.* (2018) reported that *dpy-5* animals are sensitive to juglone stress. Juglone is a naphthoquinone with a molecular mass of 174 Da and poor solubility in water (0.052 mg/ml). Faster paralysis of *dpy-4* mutants on levamisole and decreased survival of *dpy-5* on juglone suggests that these mutants have smaller pores allowing molecules less than 240 Da to get in but keep larger molecules such as Hoechst 33258 and ivermectin out. Thus, cuticle permeability for different chemicals might depend on the size and perhaps also on water solubility and other properties of the compound.

In mammalian skin, stratum corneum (SC) of the skin act as an impermeable barrier against exogenous toxins. Thin skin in the dorsum of the hand is more permeable than the palm (Sandby-Møller *et al.* 2003; Oltulu *et al.* 2018) suggesting

differential permeability of human skin. Skin barrier defects have been associated with a number of human diseases such as Gaucher's disease, atopic dermatitis, and psoriasis (Yoshiike *et al.* 1993; Holleran *et al.* 1994; Proksch *et al.* 2008; Cork *et al.* 2009; Sano 2015), and often associated with inflammation (Roberson and Bowcock 2010; Boguniewicz and Leung 2011). *Caenorhabditis elegans* can serve as a model organism to study skin's response to the infiltration of exogenous toxins such as commonly used herbicides and pesticides. Mutants of PD collagens and transcription factors can further be used to study wound healing in the skin, keloid formation, and fibrosis.

Funding

This work was supported by the Wellcome Trust/DBT India Alliance Intermediate Fellowship (Grant No. IA/I/13/1/500919) awarded to V.S. We also acknowledge support from DBT-IISc Partnership Program (BT/ PR27952/INF/22/212/2018) and infrastructure support from DST-FIST.

Conflicts of interest

None declared.

Acknowledgments

Some *C. elegans* strains were provided the CGC which is funded by the NIH Office of Infrastructure Programs (P40 OD01440).
A.S. and V.S. conceptualized the project. A.S., D.B., R.S., and S.T. performed the experiments. A.S., D.B., R.S., S.T., and V.S. analyzed the data and interpreted the results. A.S. and V.S. wrote the manuscript.

Literature cited

An JH, Blackwell TK. 2003. SKN-1 links *C. elegans* mesendodermal specification to a conserved oxidative stress response. Genes Dev. 17:1882–1893.

Atchison WD, Geary TG, Manning B, VandeWaa EA, Thompson DP. 1992. Comparative neuromuscular blocking actions of levamisole and pyrantel-type anthelmintics on rat and gastrointestinal nematode somatic muscle. Toxicol Appl Pharmacol. 112: 133–143.

Beck CD, Rankin CH. 1995. Heat shock disrupts long-term memory consolidation in *Caenorhabditis elegans*. Learn Mem. 2:161–177.

Birben E, Sahiner UM, Sackesen C, Erzurum S, Kalayci O. 2012. Oxidative stress and antioxidant defense. World Allergy Organ J. 5:9–19.

Boguniewicz M, Leung DYM. 2011. Atopic dermatitis: a disease of altered skin barrier and immune dysregulation. Immunol Rev. 242: 233–246.

Brenner S. 1974. The genetics of *Caenorhabditis elegans*. Genetics 77: 71–94.

Brunquell J, Morris S, Lu Y, Cheng F, Westerheide SD. 2016. The genome-wide role of HSF-1 in the regulation of gene expression in *Caenorhabditis elegans*. BMC Genomics. 17:1–18.

Bus J, Cagen S, Olgaard M, Gibson J. 1976. A mechanism of paraquat toxicity in mice and rats. Toxicol Appl Pharmacol. 35:501–513.

Bus J, Gibson J. 1984. Paraquat: model for oxidant-initiated toxicity. Environ Health Perspect. 55:37–46.

Cheng Y, Hercules DM. 2001. Studies of pesticides by collision-induced dissociation, postsource-decay, matrix-assisted laser desorption/ionization time of flight mass spectrometry. J Am Soc Mass Spectrom. 12:590–598.

Chisholm AD. 2015. Epidermal wound healing in the nematode *Caenorhabditis elegans*. Adv Wound Care (New Rochelle). 4: 264–271.

Chisholm AD, Hsiao TI. 2012. The *Caenorhabditis elegans* epidermis as a model skin. I: development, patterning, and growth. Wires Dev Biol. 1:861–878.

Cork MJ, Danby SG, Vasilopoulos Y, Hadgraft J, Lane ME, *et al.* 2009. Epidermal barrier dysfunction in atopic dermatitis. J Invest Dermatol. 129:1892–1908.

Cox GN, Hirsh D. 1985. Stage-specific patterns of collagen gene expression during development of *Caenorhabditis elegans*. Mol Cell Biol. 5:363–372.

Cox GN, Kramer JM, Hirsh D. 1984. Number and organization of collagen genes in *Caenorhabditis elegans*. Mol Cell Biol. 4:2389–2395.

Cox GN, Kusch M, DeNevi K, Edgar RS. 1981a. Temporal regulation of cuticle synthesis during development of *Caenorhabditis elegans*. J Cell Biol. 84:277–285.

Cox GN, Kusch M, Edgar R. 1981b. Cuticle of *Caenorhabditis elegans*: its isolation and partial characterization. J cell Biol. 90:7–17.

Cox GN, Laufer JS, Kusch M, Edgar RS. 1980. Genetic and phenotypic characterization of roller mutants of *Caenorhabditis elegans*. Genetics. 95:317–339.

Dodd W, Tang L, Lone J, Christophe Wimberly K, Wu C, Wei, *et al.* 2018. A damage sensor associated with the cuticle coordinates three core environmental stress responses in *Caenorhabditis elegans*. Genetics. 208:1467–1482.

Essmann CL, Elmi M, Shaw M, Anand GM, Pawar VM, Srinivasan MA. 2017. In-vivo high resolution AFM topographic imaging of *Caenorhabditis elegans* reveals previously unreported surface structures of cuticle mutants. Nanomed Nanotechnol Biol Med. 13:183–189.

Ewald CY, Landis JN, Abate JP, Murphy CT, Keith T. 2015. Dauer-independent insulin/IGF-1-signalling implicates collagen remodelling in longevity. Nature. 519:97–101.

Fay DS. 2005–2018. Classical genetic methods. In: WormBook: The Online Review of C. elegans Biology. Pasadena (CA): WormBook

Fernando T, Flibotte S, Xiong S, Yin J, Yzeiraj E, *et al.* 2011. *C. elegans* ADAMTS ADT-2 regulates body size by modulating TGFβ signaling and cuticle collagen organization. Dev Biol. 352:92–103.

Fraser AG, Kamath RS, Zipperlen P, Martinez-Campos M, Sohrmann M, *et al.* 2000. Functional genomic analysis of *C. elegans* chromosome I by systematic RNA interference. Nature. 408:325–330.

Gage JC. 1968. The action of paraquat and diquat on the respiration of liver cell fractions. Biochem J. 109:757–761.

Holleran WM, Ginns EI, Menon GK, Grundmann JU, Fartasch M, *et al.* 1994. Consequences of beta-glucocerebrosidase deficiency in epidermis. Ultrastructure and permeability barrier alterations in Gaucher disease. J Clin Invest. 93:1756–1764.

Honda Y, Honda S. 1999. The *daf-2* gene network for longevity regulates oxidative stress resistance and Mn-superoxide dismutase gene expression in *Caenorhabditis elegans*. FASEB J. 13:1385–1393.

Hsu AL, Murphy CT, Kenyon C. 2003. Regulation of aging and age-related disease by DAF-16 and heat-shock factor. Science. 300:1142–1145.

Hu Q, D'Amora DR, MacNeil LT, Walhout AJ, Kubiseski TJ. 2017. The oxidative stress response in *Caenorhabditis elegans* requires the GATA transcription factor ELT-3 and SKN-1/Nrf2. Genetics. 206: 1909–1922.

Hyun M, Kim J, Dumur C, Schroeder FC, You YJ. 2016. BLIMP-1/BLMP-1 and metastasis-associated protein regulate stress resistant development in *Caenorhabditis elegans*. Genetics. 203:1721–1732.

Johnstone LL. 1994. The cuticle of the nematode *Caenorhabditis elegans*: a complex collagen structure. Bioessays. 16:171–178.

Johnstone IL. 2000. Cuticle collagen genes-expression in *Caenorhabditis elegans*. Trends Genet. 16:21–27.

Kage-Nakadai E, Kobuna H, Kimura M, Gengyo-Ando K, Inoue T, *et al.* 2010. Two very long chain fatty acid acyl-CoA synthetase genes, *acs-20* and *acs-22*, have roles in the cuticle surface barrier in *Caenorhabditis elegans*. PLoS One. 5:e8857.

Kamath RS, Martinez-Campos M, Zipperlen P, Fraser AG, Ahringer J. 2001. Effectiveness of specific RNA-mediated interference through ingested double-stranded RNA in *Caenorhabditis elegans*. Genome Biol. 2:RESEARCH0002.1-0002.10.

Kass IS, Wangt CC, Walrond JP, Stretton A0W. 1980. Avermectin Bia, a paralyzing anthelmintic that affects interneurons and inhibitory motoneurons in Ascaris. Neurobiology. 77:6211–6215.

Keaney M, Matthijssens F, Sharpe M, Vanfleteren J, Gems D. 2004. Superoxide dismutase mimetics elevate superoxide dismutase activity in vivo but do not retard aging in the nematode *Caenorhabditis elegans*. Free Radic Biol Med. 37:239–250.

Kramer JM. 1994. Structures and functions of collagens in *Caenorhabditis elegans*. FASEB J. 8:329–336.

Kusch M, Edgar RS. 1986. Genetic studies of unusual loci that affect body shape of the nematode *Caenorhabditis elegans* and may code for cuticle structural proteins. Genetics. 113:621–639.

Lamitina ST, Huang CG, Strange K. 2006. Genome-wide RNAi screening identifies protein damage as a regulator of osmoprotective gene expression. Proc Natl Acad Sci U S A. 103:12173–12178.

Lamitina ST, Morrison R, Moeckel GW, Strange K. 2004. Adaptation of the nematode *Caenorhabditis elegans* to extreme osmotic stress. Am J Physiol Cell Physiol. 286:785–791.

Lewis JA, Wu CH, Berg H, Levine JH. 1980. The genetics of levamisole resistance in the nematode *Caenorhabditis elegans*. Genetics. 95: 905–928.

Lithgow GJ, White TM, Melov S, Johnson TE. 1995. Thermotolerance and extended life-span conferred by single-gene mutations and induced by thermal stress. Proc Natl Acad Sci U S A. 92: 7540–7544.

Livak KJ, Schmittgen TD. 2001. Analysis of relative gene expression data using real-time quantitative PCR and the $2^{-\Delta\Delta}$CT method. Methods. 25:402–408.

Madaan U, Yzeiraj E, Meade M, Clark JF, Rushlow CA, *et al.* 2018. BMP signaling determines body size via transcriptional regulation of collagen genes in *Caenorhabditis elegans*. Genetics. 210:1355–1367.

McMahon L, Muriel JM, Roberts B, Quinn M, Johnstone IL. 2003. Two sets of interacting collagens form functionally distinct substructures within a *Caenorhabdities elegans* extracellular matrix. Mol Biol Cell. 14:1366–1378.

Moribe H, Yochem J, Yamada H, Tabuse Y, Fujimoto T, *et al.* 2004. Tetraspanin protein (TSP-15) is required for epidermal integrity in *Caenorhabditis elegans*. J Cell Sci. 117:5209–5220.

Myllyharju J, Kivirikko KI. 2004. Collagens, modifying enzymes and their mutations in humans, flies and worms. Trends Genet. 20: 33–43.

Niu W, Lu ZJ, Zhong M, Sarov M, Murray JI, *et al.* 2011. Diverse transcription factor binding features revealed by genome-wide ChIP-seq in *C. elegans*. Genome Res. 21:245–254.

Novelli J, Ahmed S, Hodgkin J. 2004. Gene interactions in *Caenorhabditis elegans* define DPY-31 as a candidate procollagen C-proteinase and SQT-3/ROL-4 as its predicted major target. Genetics. 168:1259–1273.

Oh SI, Park JK, Park SK. 2015. Lifespan extension and increased resistance to environmental stressors by N-acetyl-L-cysteine in *Caenorhabditis elegans*. Clinics. 70:380–386.

Oltulu P, Ince B, Kokbudak N, Findik S, Kilinc F. 2018. Measurement of epidermis, dermis, and total skin thicknesses from six different body regions with a new ethical histometric technique. Turk J Plast Surg. 26:56–61.

Page AP, Johnstone IL. 2007. The cuticle. 2007 May 3. In: WormBook: The Online Review of C. elegans Biology. Pasadena (CA): WormBook.

Park EC, Horvitz HR. 1986. Mutations with dominant effects on the behavior and morphology of the nematode *Caenorhabditis elegans*. Genetics. 113:821–852.

Park SK, Tedesco PM, Johnson TE. 2009. Oxidative stress and longevity in *C. elegans* as mediated by SKN-1. Aging Cell. 8:258–269.

Partridge FA, Tearle AW, Gravato-Nobre MJ, Schafer WR, Hodgkin J. 2008. The *C. elegans* glycosyltransferase BUS-8 has two distinct and essential roles in epidermal morphogenesis. Dev Biol. 317: 549–559.

Proksch E, Brandner JM, Jensen JM. 2008. The skin: an indispensable barrier. Exp Dermatol. 17:1063–1072.

Pujol N, Cypowyj S, Ziegler K, Millet A, Astrain A, *et al.* 2008a. Distinct innate immune responses to infection and wounding in the *C. elegans* epidermis. Curr Biol. 18:481–489.

Pujol N, Zugasti O, Wong D, Couillault C, Kurz CL, *et al.* 2008b. Anti-fungal innate immunity in *C. elegans* is enhanced by evolutionary diversification of antimicrobial peptides. PLoS Pathog. 4:e1000105.

Roberson ED, Bowcock AM. 2010. Psoriasis genetics: breaking the barrier. Trends Genet. 26:415–423.

Rodriguez M, Snoek LB, De Bono M, Kammenga JE. 2013. Worms under stress: *C. elegans* stress response and its relevance to complex human disease and aging. Trends Genet. 29:367–374.

Rohlfing AK, Miteva Y, Hannenhalli S, Lamitina T. 2010. Genetic and physiological activation of osmosensitive gene expression mimics transcriptional signatures of pathogen infection in *C. elegans*. PLoS One. 5:e9010.

Sandby-Møller J, Poulsen T, Wulf HC. 2003. Influence of epidermal thickness, pigmentation and redness on skin autofluorescence. Photochem Photobiol. 77:616.

Sano S. 2015. Psoriasis as a barrier disease. Dermatol Sin. 33:64–69.

Savage-Dunn C, Padgett RW. 2017. The TGF-β family in *Caenorhabditis elegans*. Cold Spring Harb Perspect Biol. 9:a022178.

Schultz RD, Bennett EE, Ellis EA, Gumienny TL. 2014. Regulation of extracellular matrix organization by BMP signaling in *Caenorhabditis elegans*. PLoS One. 9:e101929.

Sellegounder D, Liu Y, Wibisono P, Chen CH, Leap D, *et al.* 2019. Neuronal GPCR NPR-8 regulates *C. elegans* defense against pathogen infection. Sci Adv. 5:1–16.

Shaw WM, Luo S, Landis J, Ashraf J, Murphy CT. 2007. The *C. elegans* TGF-β Dauer pathway regulates longevity via insulin signaling. Curr Biol. 17:1635–1645.

Shemer G, Suissa M, Kolotuev I, Nguyen KC, Hall DH, *et al.* 2004. EFF-1 is sufficient to initiate and execute tissue-specific cell fusion in *C. elegans*. Curr Biol. 14:1587–1591.

Stepek G, McCormack G, Page AP. 2010. Collagen processing and cuticle formation is catalysed by the astacin metalloprotease DPY-31 in free-living and parasitic nematodes. Int J Parasitol. 40:533–542.

Styer KL, Singh V, Macosko E, Steele SE, Bargmann CI, *et al.* 2008. Innate immunity in *Caenorhabditis elegans* is regulated by neurons expressing NPR-1/GPCR. Science 322:460–465.

Taffoni C, Pujol N. 2015. Mechanisms of innate immunity in *C. elegans* epidermis. Tissue Barriers. 3:e1078432.

Teuscher AC, Jongsma E, Davis MN, Statzer C, Gebauer JM, Naba A, *et al.* 2019. The in-silico characterization of the *Caenorhabditis elegans* matrisome and proposal of a novel collagen classification. Matrix Biol Plus. 1:100001.

Thein MC, Mccormack G, Winter AD, Johnstone IL, Shoemaker CB, *et al.* 2003. *Caenorhabditis elegans* exoskeleton collagen COL-19: an adult-specific marker for collagen modification and assembly, and the analysis of organismal morphology. Dev Dyn. 226:523–539.

Thor H, Moldeus P, Orrenius S. 1979. Metabolic activation and hepatotoxicity: effect of cysteine, N-acetylcysteine, and methionine on glutathione biosynthesis and bromobenzene toxicity in isolated rat hepatocytes. Arch Biochem Biophys. 192:405–413.

Tullet JM, Hertweck M, An JH, Baker J, Hwang JY, Liu S, *et al.* 2008. Direct inhibition of the longevity promoting factor SKN-1 by insulin-like signaling in *C. elegans*. Cell. 132:1025–1038.

Wang J, Tokarz R, Savage-Dunn C. 2002. The expression of TGFβ signal transducers in the hypodermis regulates body size in *C. elegans*. Development. 129:4989–4998.

Wheeler JM, Thomas JH. 2006. Identification of a novel gene family involved in osmotic stress response in *Caenorhabditis elegans*. Genetics. 174:1327–1336.

Winter AD, McCormack G, Page AP. 2007. Protein disulfide isomerase activity is essential for viability and extracellular matrix formation in the nematode *Caenorhabditis elegans*. Dev Biol. 308:449–461.

Wolff S, Ma H, Burch D, Maciel GA, Hunter T, *et al.* 2006. SMK-1, an essential regulator of DAF-16-mediated longevity. Cell. 124: 1039–1053.

Wu CW, Wang Y, Choe KP. 2017. F-box protein XREP-4 is a new regulator of the oxidative stress response in *C. elegans*. Genetics. 206: 859–871.

Yin J, Madaan U, Park A, Aftab N, Savage-Dunn C. 2015. Multiple cis elements and GATA factors regulate a cuticle collagen gene in *C. elegans*. Genesis. 53:278–284.

Yoshiike T, Aikawa Y, Sindhvananda J, Suto H, Nishimura K, *et al.* 1993. Skin barrier defect in atopic dermatitis: increased permeability of the stratum corneum using dimethyl sulfoxide and theophylline. J Dermatol Sci. 5:92–96.

Zugasti O, Bose N, Squiban B, Belougne J, Kurz CL, *et al.* 2014. Activation of a G protein-coupled receptor by its endogenous ligand triggers the innate immune response of *Caenorhabditis elegans*. Nat Immunol. 15:833–838.

Communicating Editor: B. Grant